Vertical profiles of aerosol volume from high spectral resolution infrared transmission measurements: Results

Annmarie Eldering,[1,2] Brian H. Kahn,[3] Franklin P. Mills,[3,4] Fredrick W. Irion,[1] Helen M. Steele,[3,5] and Michael R. Gunson[1]

Received 10 February 2004; revised 2 June 2004; accepted 23 July 2004; published 19 October 2004.

[1] The high-resolution infrared absorption spectra of the Atmospheric Trace Molecule Spectroscopy (ATMOS) experiment are utilized to derive vertical profiles of sulfate aerosol volume density and extinction coefficient. Following the eruption of Mt. Pinatubo in June 1991, the ATMOS spectra obtained on three Space Shuttle missions (1992, 1993, and 1994) provide a unique opportunity to study the global stratospheric sulfate aerosol layer shortly after a major volcanic eruption and periodically during the decay phase. Synthetic sulfate aerosol spectra are fit to the observed spectra, and a global fitting inversion routine is used to derive vertical profiles of sulfate aerosol volume density. Vertical profiles of sulfate aerosol volume density for the three missions over portions of the globe are presented, with the peak in aerosol volume density occurring from as low as 10 km (polar latitudes) to as high as 20 km (subtropical latitudes). Derived aerosol volume density is as high as 2–3.5 μm^3 cm^{-3} ±10% in 1992, decreasing to 0.2–0.5 μm^3 cm^{-3} ±20% in 1994, in agreement with other experiments. Vertical extinction profiles derived from ATMOS are compared with profiles from Improved Stratospheric And Mesospheric Sounder (ISAMS) and Cryogenic Limb Array Etalon Spectrometer (CLAES) that coincide in space and time and show good general agreement. The uncertainty of the ATMOS vertical profiles is similar to CLAES and consistently smaller than ISAMS at similar altitudes. *INDEX TERMS:* 0305 Atmospheric Composition and Structure: Aerosols and particles (0345, 4801); 0340 Atmospheric Composition and Structure: Middle atmosphere—composition and chemistry; 1640 Global Change: Remote sensing; *KEYWORDS:* stratospheric aerosol, Mt. Pinatubo

Citation: Eldering, A., B. H. Kahn, F. P. Mills, F. W. Irion, H. M. Steele, and M. R. Gunson (2004), Vertical profiles of aerosol volume from high spectral resolution infrared transmission measurements: Results, *J. Geophys. Res.*, *109*, D20201, doi:10.1029/2004JD004623.

1. Introduction

[2] Observations of stratospheric sulfuric acid aerosols were reported from a wide range of observing platforms after the eruption of Mt. Pinatubo in 1991 [*Ackerman and Strabala*, 1994; *Deshler et al.*, 1993; *Grainger et al.*, 1995, 1993; *Hervig and Deshler*, 1998; *Hervig et al.*, 1996; *Lambert et al.*, 1993, 1997, 1996b; *Massie et al.*, 1996a; *Russell et al.*, 1996; *Steele et al.*, 2003]. From this wide variety of observing platforms, a picture of the aerosol size, composition, and aerosol volume density has been assembled. An excellent overview of the Pinatubo aerosol observations is presented in the work of *Russell et al.* [1996] where data from space, air and ground based measurements (primarily in the visible and midinfrared) are analyzed and combined.

[3] *Lambert et al.* [1997] discuss the global evolution of the Mt. Pinatubo aerosol composition and volume density from a combination of infrared and microwave remote sensing measurements. To examine composition, they combined temperature measurements of Improved Stratospheric And Mesospheric Sounder (ISAMS) and Cryogenic Limb Array Etalon Spectrometer (CLAES) with water vapor measurements from MLS, and found equilibrium composition varied from 50% sulfuric acid by weight in the lowest layers (15 km at the equator) to 80% in higher layers (polar regions and above 27 km at the equator). As described in the work of *Lambert et al.* [1996a] and *Grainger et al.* [1995], aerosol extinction at 12.11 μm is retrieved from ISAMS and converted to effective radius, surface area density, and volume density. The extinction values are determined to 20 to 25% precision, and the uncertainty in the aerosol volume density is at least this large. These analyses report aerosol sulfate mass densities ranging from 10 $\mu g\ m^{-3}$ in October 1991 to 0.5 $\mu g\ m^{-3}$ in March 1993.

[1]Jet Propulsion Laboratory, California Institute of Technology, Pasadena, California, USA.
[2]Also at Department of Atmospheric and Oceanic Sciences, University of California at Los Angeles, Los Angeles, California, USA.
[3]Department of Atmospheric and Oceanic Sciences, University of California at Los Angeles, Los Angeles, California, USA.
[4]Now at Centre for Resource and Environmental Studies, Australian National University, Canberra, ACT, Australia.
[5]Also at Department of Geography, California State University at Northridge, Northridge, California, USA.

0148-0227/04/2004JD004623$09.00

[4] In a unique analysis of multiwavelength infrared measurements, *Massie et al.* [1994] derived an ad hoc empirical quantity based on the CLAES aerosol extinction at 925, 1257, and 1605 cm^{-1} to distinguish between sulfate aerosol and polar stratospheric clouds. This quantity is based on the area of a triangle in wave number-aerosol extinction space. They then demonstrated the success of this spectral separation through a comparison with separation based on thermodynamic arguments.

[5] Analysis of the ATMOS measurements to determine stratospheric aerosol composition, size, and density have also been reported by *Zasetsky et al.* [2002]. Aimed at developing an extremely fast computational technique, this analysis applied a very different method than is used here for separating the gas and aerosol signatures. They used wavelet analysis and attributed the low frequency portion of the spectra to aerosols. Results from analysis of the northern latitude measurements of 1992 and a subset of the measurements made in 1994 by ATMOS are reported as average vertical profiles of aerosol volume density and effective radius with estimated uncertainties on the order of 40%. ATMOS spectra also have been used to analyze broad extinction features produced by post-Pinatubo sulfate [*Eldering et al.*, 2001; *Rinsland et al.*, 1994], and cloud cover in the upper troposphere [*Kahn et al.*, 2002; *Rinsland et al.*, 1998].

[6] In this paper we retrieve vertical profiles of stratospheric sulfuric acid aerosol volume density from the high-resolution (0.01 cm^{-1}) infrared solar occultation absorption spectra derived from ATMOS measurements. These measurements were taken as part of the Atmospheric Laboratory for Applications and Science (ATLAS) during approximately 10 day periods in March 1992, April 1993, and November 1994 [*Gunson et al.*, 1996; *Kaye and Miller*, 1996]. Spectra are taken in several band-pass filters from 600 to 4750 cm^{-1} [*Irion et al.*, 2002], and each spectral subregion has a different sensitivity to aerosol composition and size [*Echle et al.*, 1998; *Eldering et al.*, 2001; *Steele et al.*, 2003]. We briefly review the method employed here to derive vertical profiles of aerosol volume density and the associated uncertainty from measured ATMOS spectra, present examples that illustrate the temporal changes observed in post-Pinatubo stratospheric aerosols, and compare the results from our analysis of ATMOS spectra with those obtained by previous studies using CLAES and ISAMS data. This work provides a complete picture of stratospheric sulfuric acid aerosols as measured by ATMOS and results in smaller uncertainties on the aerosol volume density than previously reported results.

2. Methodology

[7] Vertical profiles of aerosol volume density were derived from the spectra measured by ATMOS during an infrared solar occultation via a four step process. First, the line of sight absorption due to gas phase species was determined. The results presented here used the ATMOS version 3 gas volume mixing ratios [*Irion et al.*, 2002] rather than determining the gas profile that best fit the ATMOS measurements within each 2 cm^{-1} window [*Eldering et al.*, 2001]. Second, line of sight residual continuum spectra are derived from the measured ATMOS spectra and the transmission spectra calculated using a forward model and the gas volume mixing ratios. Third, the line of sight residual continuum spectra are compared to modeled aerosol spectra to derive the line of sight aerosol slant volume. Finally, a geometric global inversion derives a vertical profile of the aerosol volume density from the aerosol slant volumes for each occultation.

2.1. Residual Continuum Spectrum

[8] The residual continuum spectrum which comprises the total transmission, $T(\nu, z')$, reduced by that part attributed to gases, is given by $K_{\mathrm{meas}}(\nu, z')$ at a frequency ν along a path through tangent altitude z'. This is shown in equation (1):

$$K_{meas}(\nu, z') = \frac{T(\nu, z')}{\exp\left[-\sum_j \left\{\int_x \kappa_j(\nu, x) g_j(x) dx\right\}\right]}, \quad (1)$$

where κ_j, is the absorption coefficient at frequency ν and g_j is the number density of gas j along an optical slant path, x, with tangent altitude z'. Operationally, a linear approximation to $K_{meas}(\nu, z')$ for each 2 cm^{-1} window is retrieved. For the aerosol analysis presented here, the gas profiles were held constant while the mean value and slope of the line approximating the continuum level within each 2 cm^{-1} window were retrieved by minimizing the RMS error in the fit [*Norton and Rinsland*, 1991; *Rodgers*, 1990]. The set of mean values of the continuum level is reported as $K_{meas}(\nu, z')$.

[9] For the analysis reported here, data from three ATMOS filters (1, 9, and 12) that contain the spectral regions of interest for determining stratospheric sulfuric acid aerosol volume density and composition were selected. Infrared spectra are primarily sensitive to composition in the 800–3000 cm^{-1} region where the imaginary refractive index of sulfuric acid is large and therefore absorption dominates scattering [*Echle et al.*, 1998; *Eldering et al.*, 2001; *Steele et al.*, 2003]. At wave numbers of 3700 cm^{-1} and larger the imaginary refractive index is quite small and size-dependent scattering effects become more important. The spectral band passes of the ATMOS filters vary, and there are terms in the error budget that are filter-dependent. To create the most consistent set of data to use in this analysis, we have selected spectral regions that contain sulfuric acid spectral features and are nearly common to three filters. Data from the 820–992 cm^{-1} region were used for all three filters, data from the 1072–1240 cm^{-1} region were used for filters 9 and 12, and data from the 1072–1190 cm^{-1} region were used for filter 1. Filter 1 data end at 1190 cm^{-1} so data at higher frequencies are not available in that filter. The region between 992 and 1072 cm^{-1} is in the heart of an ozone absorption band which makes it impossible to extract the aerosol signature, so it is not included in the aerosol fitting. Beyond 1240 cm^{-1}, the collision-induced oxygen absorption feature is significant, and even use of the most recent absorption coefficients [*Thibault et al.*, 1997] results in large errors in the determination of the continuum level. There is a strong water absorption feature that limits our

ability to determine the aerosol signature in a wide region around 1600 cm^{-1}.

2.2. Aerosol Model Fitting

[10] The best fit aerosol slant volume, $V(z')$, is found by performing a nonlinear least squares fit between $K_{meas}(\nu, z')$ and synthetic aerosol transmission spectra, $K_{model}(\nu, z')$ [*Eldering et al.*, 2001]. The synthetic aerosol transmission spectra depend on the modeled aerosol extinction coefficients, $k_{ext}(\nu, z')$, as shown in equation (2):

$$K_{model}(\nu, z') = \mathrm{C}\ \exp[-k_{ext}(\nu, z') \cdot V(z')], \quad (2)$$

where C is a scaling factor relating to the nonlinearity of the ATMOS instrument [*Kahn et al.*, 2002]. The calculation of $k_{ext}(\nu, z')$ is discussed in more detail below. As discussed in the work of *Kahn et al.* [2002], the synthetic transmission spectra may include terms for both aerosols and clouds. The best fit is determined using a chi-square minimization:

$$\chi^2 = 1/(\mathrm{N}-1)\Sigma_i[[K_{meas}(\nu_i, z') - K_{model}(\nu_i, z')]/\sigma(\nu_i)]^2, \quad (3)$$

where N is the number of spectral points, $K_{model}(\nu_i, z')$ is the synthetic aerosol transmission spectrum at frequency ν_i, and $\sigma(\nu_i)$ is the uncertainty in the continuum level at that frequency. A single χ^2 is calculated for each spectrum by combining the two spectral regions when calculating χ^2. This spectral fitting is performed for each spectrum taken in an occultation to determine the aerosol volume slant column at each tangent altitude in an occultation. A global geometric inversion procedure is then applied to the resulting set of aerosol volume slant columns and slant path distances (one each per tangent altitude) [*Irion et al.*, 2002] to find the vertical profile of aerosol volume density and its associated uncertainty.

[11] The aerosol model used in this analysis, $k_{ext}(\nu, z')$, is generated by Mie calculations for an aerosol size distribution representative of background stratospheric sulfuric acid aerosols (lognormal r = 0.07 μm, σ = 2.03, r_{eff} = 0.25 μm) [*Goodman et al.*, 1994; *Oberbeck et al.*, 1983] using the optical constants of *Tisdale et al.* [1998] measured at 215 K for an aerosol composition of 75% by weight sulfuric acid solution. Aerosol composition could be calculated from thermodynamic relationships using the water vapor and temperature profiles. In the altitude range of 18–24 km, the thermodynamically predicted composition varied over a rather narrow range of 74–78% with uncertainties of 3 to 4%. Preliminary tests with a number of refractive index data sets [*Biermann et al.*, 2000; *Niedziela et al.*, 1999, 1998; *Tisdale et al.*, 1998; *Toon et al.*, 1994] show that additional uncertainty in composition arises from the application of different data. A complete sensitivity analysis is the subject of a future paper.

2.3. Error Budget

[12] The error assigned to the mean value of the continuum level within each 2 cm^{-1} interval includes three components. They are related to the gas fitting error, zero level offset errors [*Abrams et al.*, 1994], and the tilt of the continuum level. The error due to gas fitting is contained in the covariance matrix [*Irion et al.*, 2002]. This uncertainty largely stems from spectroscopic parameter uncertainty for the gases. Detailed analysis was performed to determine the zero level offsets and zero level offset errors for the ATMOS filters, and it was found that the zero level offsets and errors are 0.03 ± 0.01 for filter 9, 0.002 ± 0.005 for filter 1, and 0.006 ± 0.0065 for filter 12, the three filters used for the present analysis. For tangent altitudes above the tropopause, this error term dominates the total continuum level error, although there are a few spectral regions where the gas fitting error can also contribute. For spectra with tangent altitudes well into the troposphere, gas fitting errors and the error due to the zero level offset error both contribute. The tilt term, and its associated error, is only large for those 2 cm^{-1} windows where absorption lines become saturated and have effective widths larger than the width of the windows themselves. This occurs only at very low tangent altitudes. Further discussion on the errors associated with the ATMOS measurements can be found in the work of *Irion et al.* [2002] and *Kahn et al.* [2002]. The continuum level errors are very important in analyzing our ability to retrieve accurate aerosol composition from ATMOS data. As the errors become larger, a wider set of aerosol models will fit the observations within the error and there is greater uncertainty in the retrieved vertical profiles of aerosol volume density.

3. Results

[13] Vertical profiles of aerosol volume density were retrieved for the ATMOS observations of 24 March to 3 April 1992, 8–16 March 1993, and 3–14 November 1994. Figures 1–3 show a representative sample of the retrieved profiles with uncertainties superimposed. The full set of profiles and residual continuum spectra can be found at http://atmos.jpl.nasa.gov/atmos. Figure 1 presents a set of profiles from 1992 at an assortment of latitudes, with profiles from the same region of the world clustered together. It can be seen that some profiles include the peak of the aerosol layer while others do not go below the peak. The peak concentrations range from 1 to 4 $\mu m^3\ cm^{-3}$ and occur at altitudes from 17 to 20 km. Uncertainties at these altitudes are typically 10%. The aerosol loadings are consistent with other measurements in this post-Pinatubo period. In regions with the highest sulfate loading during the 1992 and 1993 missions, the sun tracker would lose sight of the sun and the measurements would come to an abrupt end [*Irion et al.*, 2002; *Kahn et al.*, 2002]. As a result, many vertical profiles do not sample the peak of the aerosol volume density profile in the lower stratosphere. By 1994 this was no longer a problem as aerosol loadings had decreased by an order of magnitude compared to 1992. Figure 2 is a similar plot showing the 1993 measurements. The number of ATMOS observations in 1994 were much more numerous, and half of the retrieved profiles are shown in Figure 3. Of the 1994 measurements, nearly all sample through the peak of the aerosol layer reporting peak concentrations of 0.3 to 0.6 $\mu m^3\ cm^{-3}$ with uncertainties of 20%. In a number of 1994 cases, the retrieved aerosol volume density profile has a secondary maximum at an altitude above the primary peak in the profile. The peak aerosol volumes observed in 1992, and latitudinal differ-

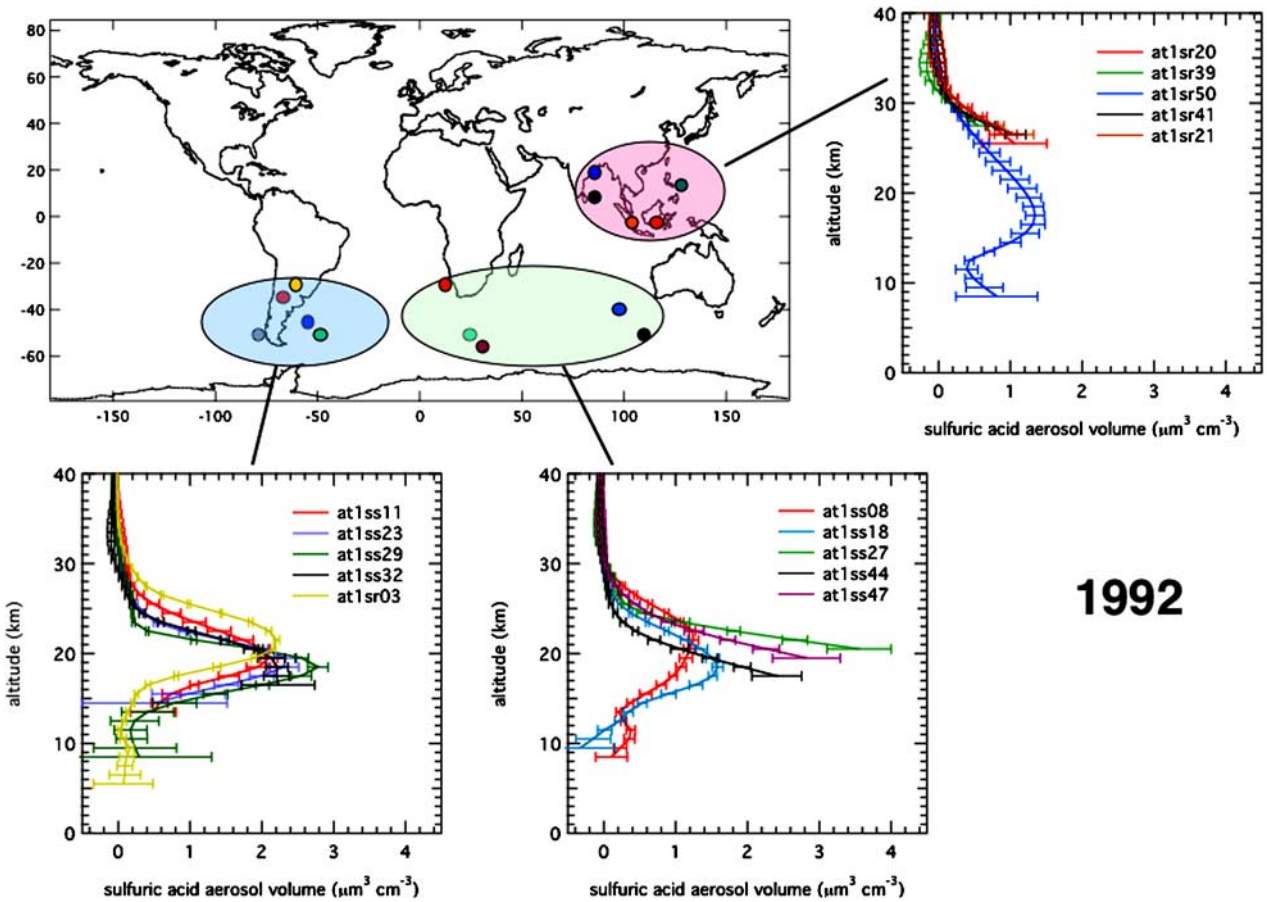

Figure 1. Profiles of aerosol volume density retrieved from ATMOS 1992 measurements.

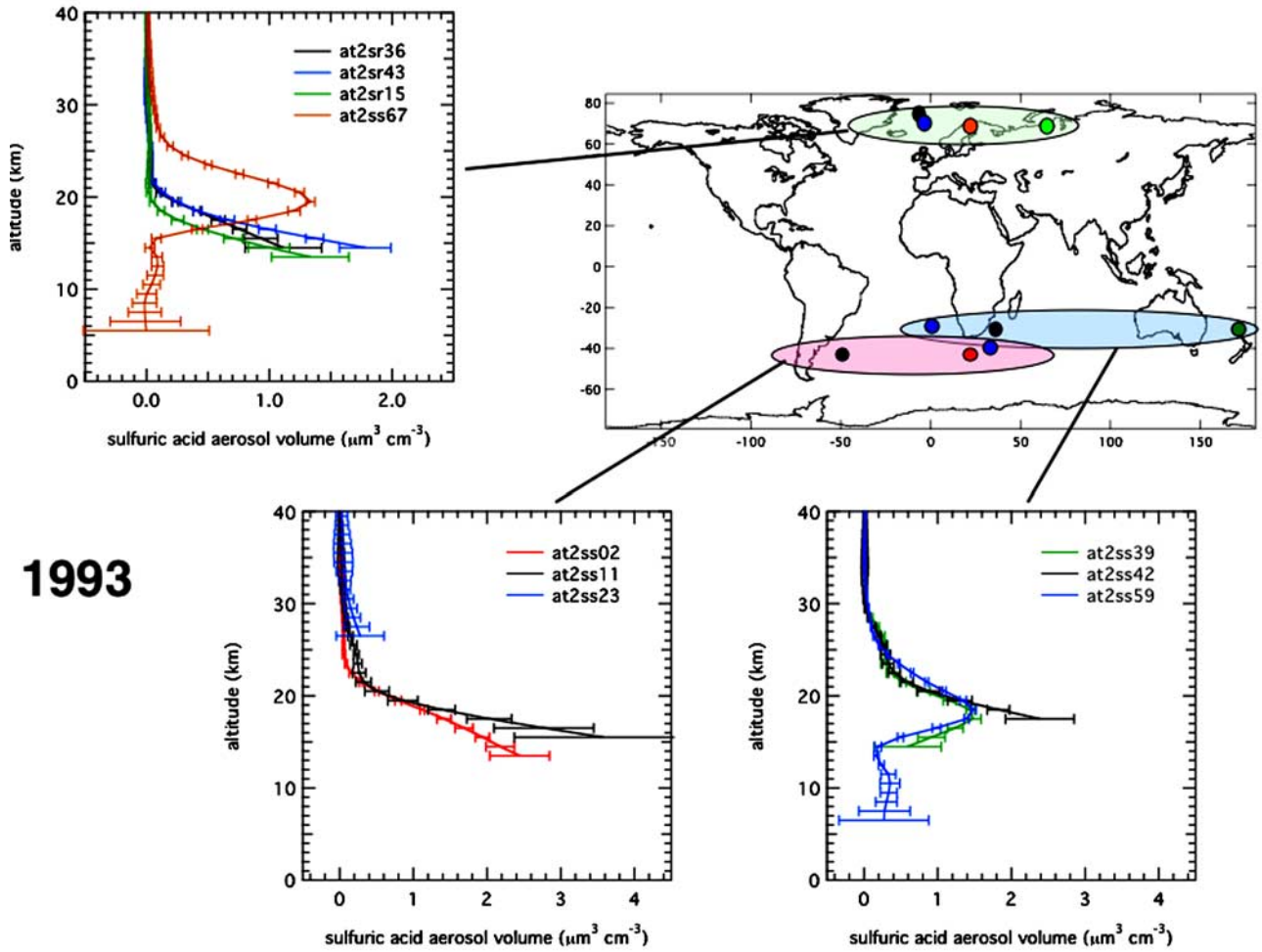

Figure 2. Profiles of aerosol volume density retrieved from ATMOS 1993 measurements.

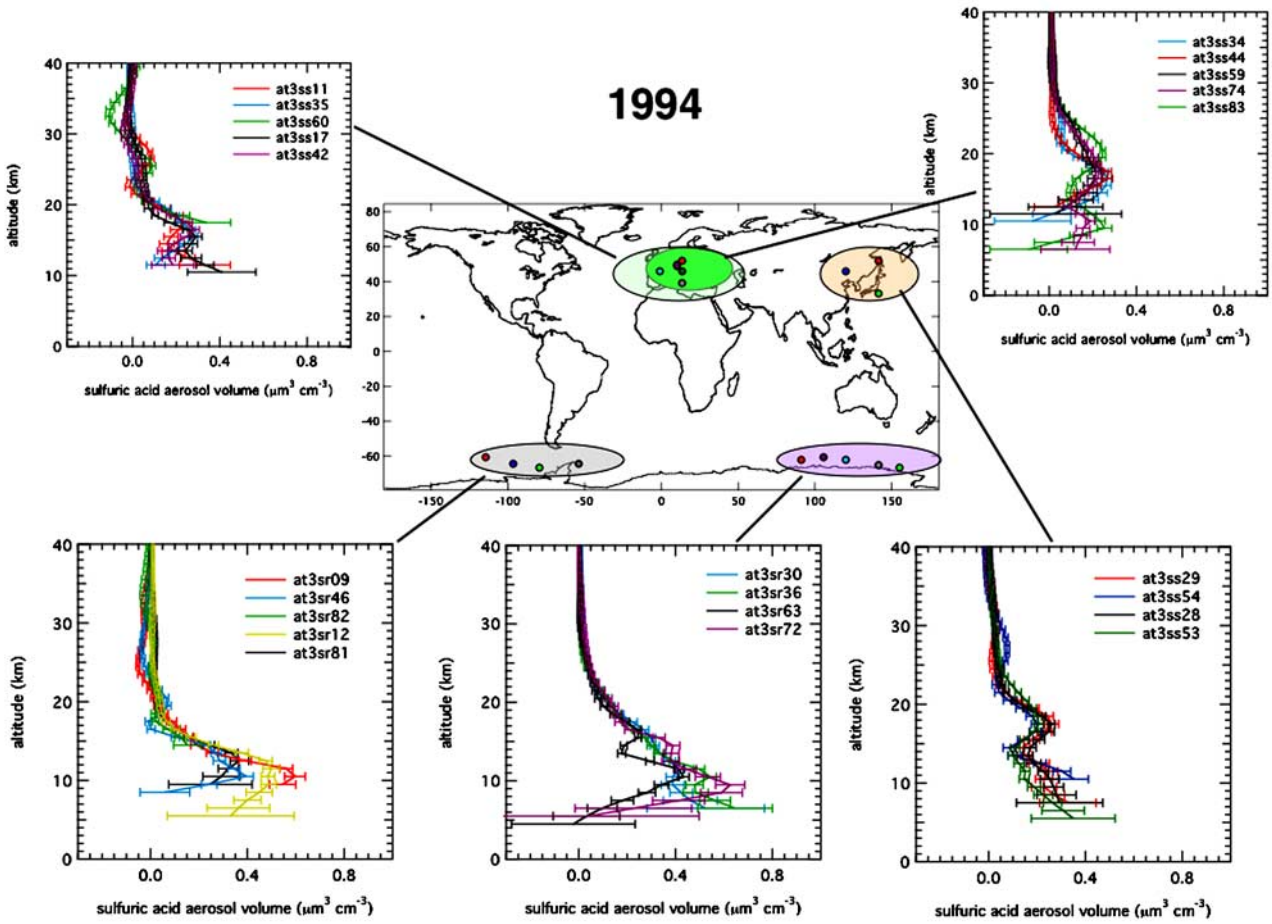

Figure 3. Profiles of aerosol volume density retrieved from ATMOS 1994 measurements.

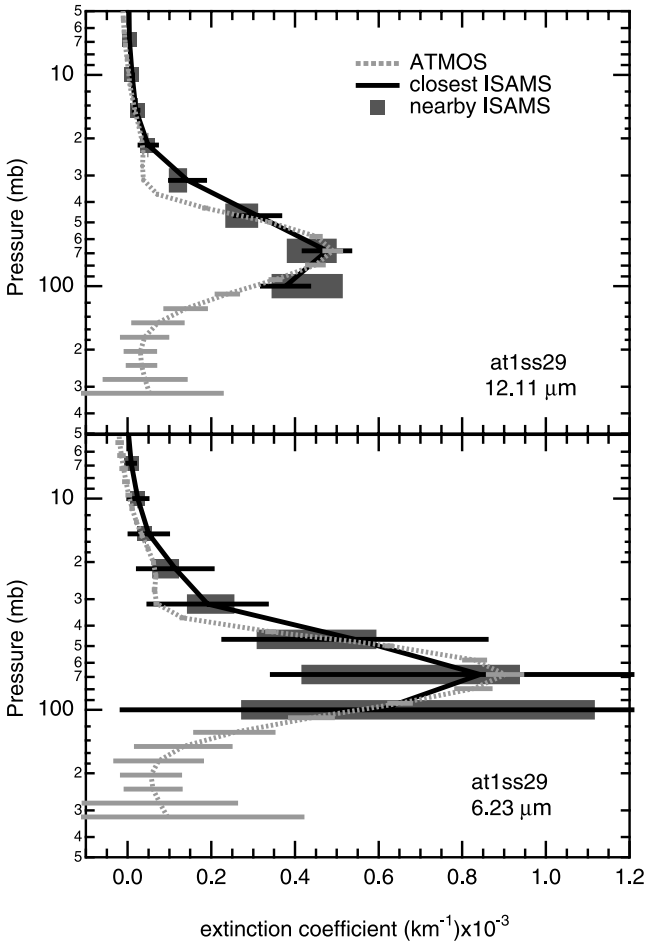

Figure 4. ISAMS aerosol extinction and ATMOS aerosol extinction at 6.23 and 12.11 μm for ATMOS occultation at1ss29. All ISAMS measurements made within 5 degrees longitude and latitude and 24 hours are reported. The gray areas show the range of the nearby ISAMS measurements.

ences in the altitude of the peak concentration reflect the variation of tropopause height with latitude.

4. Discussion

[14] Although there are not enough ATMOS measurements to develop an aerosol climatology or to make statistical comparisons with other aerosol measurements, it is possible to make comparisons with individual profiles that were taken in spatial and temporal proximity to the ATMOS measurements. Aerosol extinction coefficients retrieved from CLAES and ISAMS measurements have been reported [*Massie et al.*, 1996b]. Both CLAES and ISAMS were onboard the Upper Atmosphere Research Satellite (UARS). CLAES was a thermal emission etalon spectrometer with a number of blocker channels between 3.5 and 13 μm and aerosol extinction is reported at 790, 843, 880, and 925 cm^{-1}. ISAMS was a pressure modulated infrared radiometer that made limb measurements and reported aerosol extinction coefficients at 6.23 μm and 12.11 μm (1605 and 826 cm^{-1}, respectively). CLAES reported 461 days of data from 25 October 1991 to 5 May 1993. ISAMS made measurements on 182 days between 26 September 1991 and 29 July 1992.

[15] The quantities reported from the CLAES (version 8 of L3A data) and ISAMS (version 10 of L3A data) instruments are vertical profiles of aerosol extinction. A number of approaches have been used to convert these extinction profiles to vertical profiles of aerosol volume density and number [*Grainger et al.*, 1995, 1993; *Lambert et al.*, 1993, 1997; *Russell et al.*, 1996]. In this work, we will compare ATMOS measurements on the basis of aerosol extinction coefficients with those derived from CLAES and ISAMS measurements to eliminate potential discrepancies due to the conversion method used to derive aerosol volume density. To create a comparable quantity from the ATMOS data, we used the derived vertical profile of aerosol volume density together with the spectrally dependent aerosol extinction coefficient from our best fit aerosol model to calculate the extinction due to aerosols along the ATMOS line of sight at each wavelength of interest for each tangent height in an occultation. The error on the aerosol volume density was propagated into an error on the aerosol extinction coefficient in the same manner.

[16] In the following figures, comparisons are shown for all ATMOS occultations where at least one of the three instruments included the peak of the aerosol profile and met the coincidence criteria as described below. ISAMS and CLAES measurements were considered coincident if they were taken within 5 degrees longitude, 5 degrees latitude, and 24 hours of an ATMOS occultation. For stratospheric comparisons, this should introduce minimal differences as the stratospheric aerosol had evolved into a fairly horizontally homogeneous layer on the spatial scale of the occultation measurement (100–200 km) by the time of the ATLAS1 mission [*Russell et al.*, 1996]. Using SAGE extinction data, it has been shown that the stratospheric sulfate aerosol is much more horizontally homogeneous in spatial extent than clouds [*Kent et al.*, 1993]. Figure 4 shows a comparison of ISAMS aerosol extinction and that derived from the ATMOS measurement at1ss29 for 12.11 and 6.23 μm. In this and subsequent figures, error bars are included only on the closest ISAMS or CLAES profile for clarity. There is more similarity among the coincident ISAMS 12.11 μm measurements than among the ISAMS 6.23 μm measurements. This is also true for the other ISAMS cases that were examined for this comparison. ISAMS uncertainties at 70 mb are approximately 10–15% for the 12.11 μm measurements and 40–70% for the 6.23 μm measurements. The ISAMS data are reported on a coarser pressure grid than the ATMOS measurements, and overall have larger error bars than ATMOS data. For this ATMOS occultation, at1ss29, and coincident ISAMS observations, both ISAMS and ATMOS show a peak in the aerosol extinction at approximately 70 mb and report a very similar extinction coefficient of $\sim 4.8 \times 10^{-4}$ km^{-1} at 12.11 μm. The ATMOS extinction profile at 6.23 μm is very similar to the closest ISAMS measurement but differs by large amounts from some of the other nearby ISAMS profiles. The peak extinction in the ATMOS profile at 6.23 μm is $\sim 9.0 \times 10^{-4}$ km^{-1}, approximately twice the aerosol extinction at 12.11 μm.

[17] Figure 5 compares the ISAMS extinction at 12.11 μm for four more occultations from the ATLAS1 mission. Like

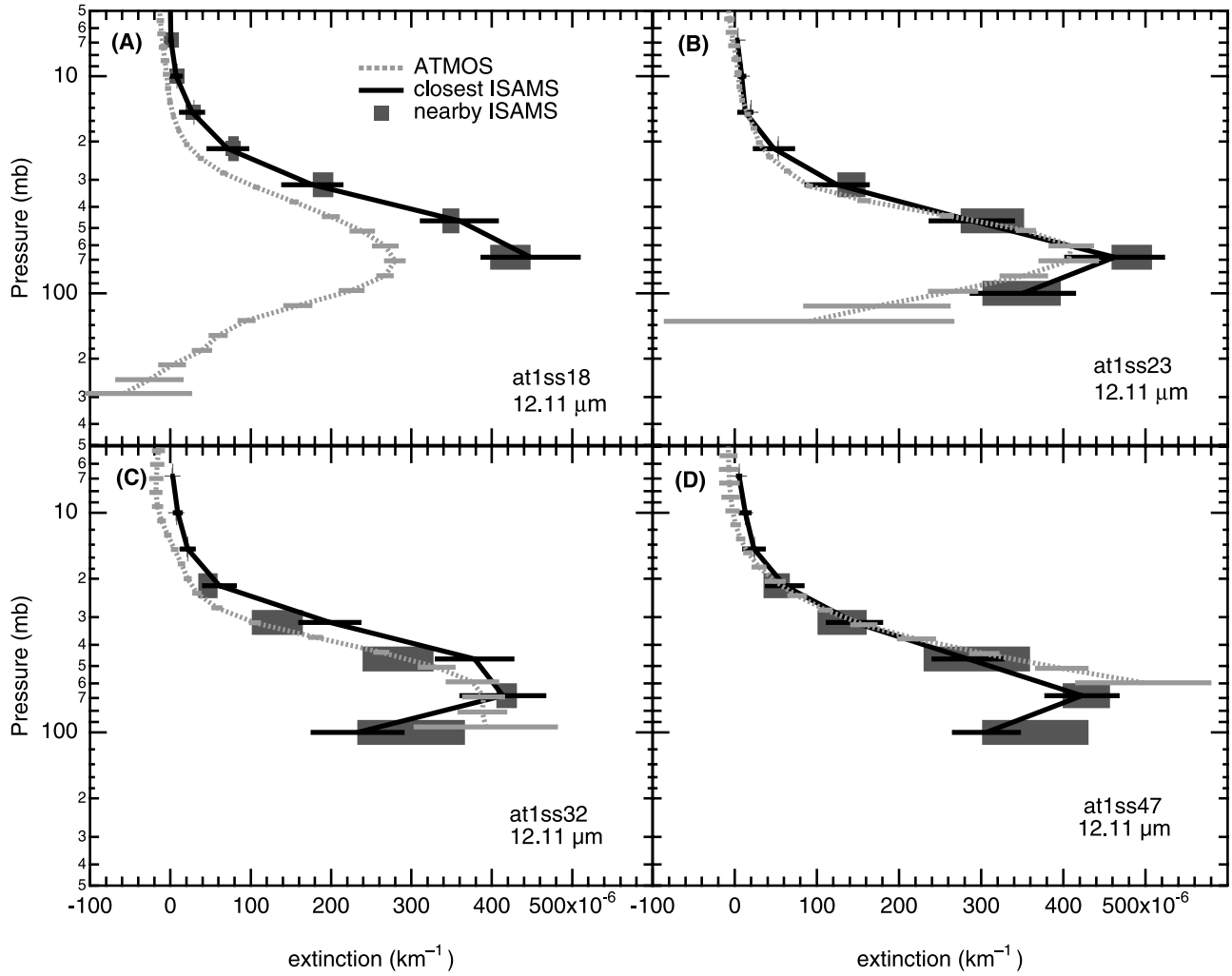

Figure 5. ISAMS aerosol extinction at 12.11 μm and ATMOS aerosol extinction for four ATMOS occultations.

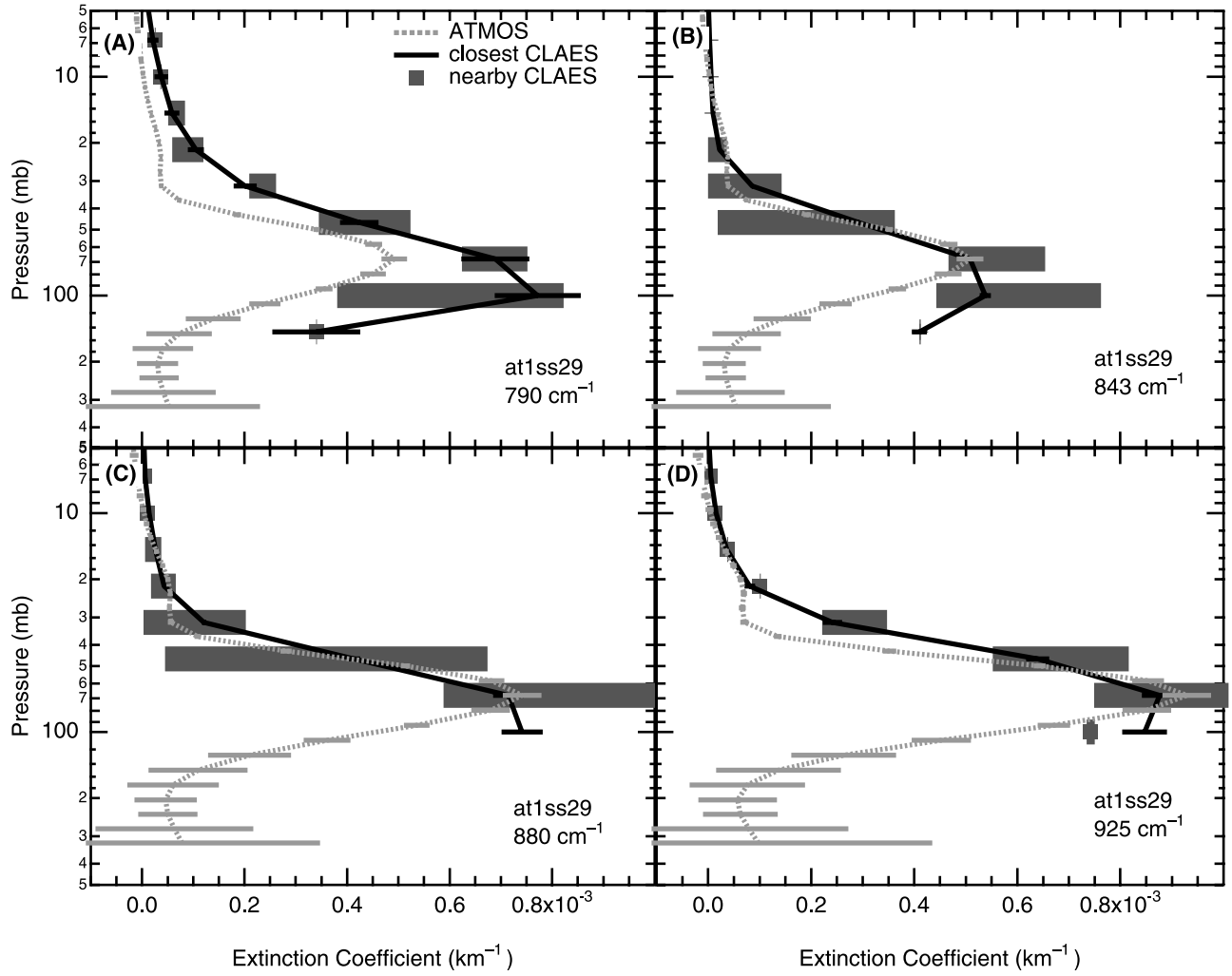

Figure 6. Comparisons of CLAES and ATMOS aerosol extinction at the four CLAES aerosol extinction channels for ATMOS occultation at1ss29.

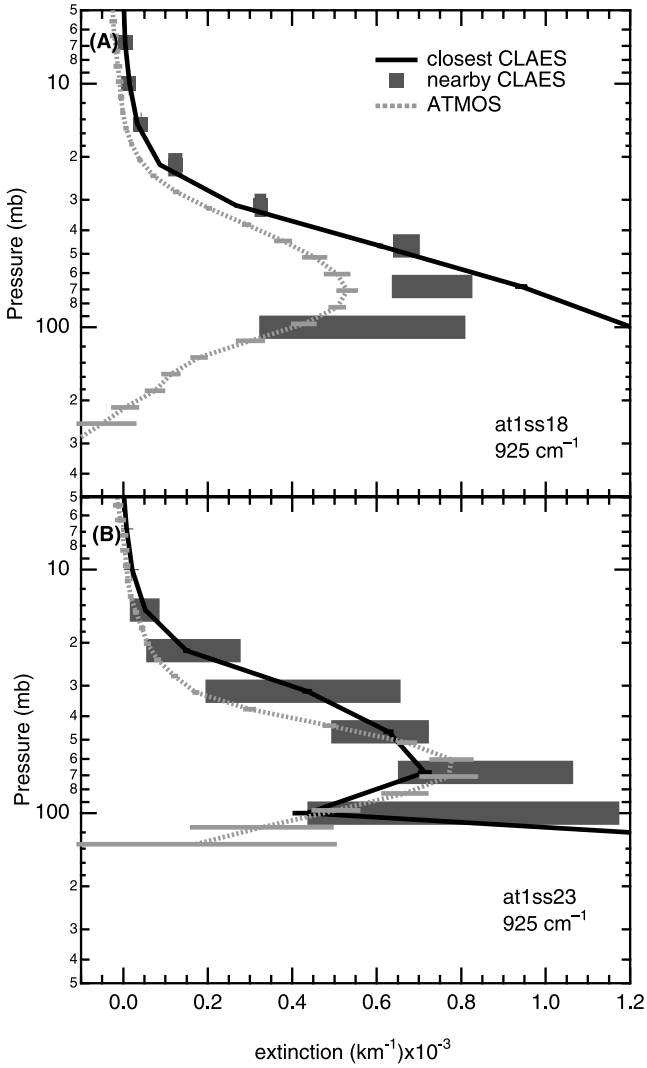

Figure 7. CLAES extinction at 925 cm^{-1} and comparable ATMOS aerosol extinction profiles.

the previous cases, there generally is good agreement between the ATMOS extinction profiles and those of ISAMS. The exception is the ATMOS occultation at1ss18, which shows considerably smaller aerosol extinction than the coincident ISAMS measurements. The ATMOS retrieval for at1ss18 found the extinction due to a cloud below 180 mb was significant, but this does not explain the differences between ATMOS and ISAMS above 100 mb.

[18] CLAES aerosol extinction profiles at four wavelengths and the comparable ATMOS data for the coincident occultation at1ss29 are shown in Figure 6. As with ISAMS, CLAES data are reported on a coarser pressure grid than ATMOS, but we see general agreement in the magnitude of the reported extinction coefficients. The ATMOS values at 790 cm^{-1} are smaller than the CLAES values but the results from the two instruments generally agree for the other three frequencies. Other comparisons (not shown here) were similar. The reported CLAES errors for 790, 843, 880, and 925 cm^{-1}, respectively, are 12%, 5%, 7%, 7%, respectively, becoming larger above 20 mb. These results are consistent with the results reported in the work of *Massie et al.* [1996b] that CLAES aerosol extinction in the 12.65 μm channel (790 cm^{-1}) is on average 30% larger than ISAMS aerosol extinction at 12.11 μm. We find that CLAES extinction at 790 cm^{-1} is larger than the ATMOS retrievals, but at other wave numbers, the CLAES and ATMOS measurements agree more closely.

[19] Figure 7 makes comparisons between ATMOS occultations and CLAES aerosol extinction at 925 cm^{-1} for two additional occultations. Again these measurements have similar uncertainties, and good agreement is seen, although the measurements do not always have overlapping error.

5. Summary and Conclusions

[20] Vertical profiles of stratospheric sulfuric acid aerosol volume density have been retrieved from the ATMOS high spectral resolution infrared solar occultation measurements made in 1992, 1993, and 1994. The peak aerosol volume densities range from 1 to 4 μm^3 cm^{-3} and occur at altitudes from 15 to 20 km in the 1992 measurements and peak at 0.3 to 0.6 μm^3 cm^{-3} at altitudes from 10 to 15 km in 1994 with uncertainties of 10% in 1992 and 20% in 1994 on aerosol volume density at the peak of the vertical profile. The results are consistent with stratospheric aerosol volume densities reported from other measurement techniques. The ATMOS measurements of aerosol extinction are also in generally good agreement with the infrared measurements by ISAMS and CLAES. In future work, the utility of high spectral resolution infrared solar occultation measurements for characterizing the aerosol composition will be discussed. The methods reported here can be applied to the ACE instrument on SciSat [*Boone and Bernath*, 2003] and any future high spectral resolution infrared solar occultation measurements.

[21] **Acknowledgments.** We would like to thank Albert Y. Chang, Geoff C. Toon, and Bhaswar Sen for many helpful discussions. This work was performed in part at the Jet Propulsion Laboratory, California Institute of Technology, under contract with NASA. A portion of the funding for this project (FPM, HMS, BHK) was provided by NASA Award NAG5-6396 and NASA New Investigator grant NAG5-8812.

References

Abrams, M. C., G. C. Toon, and R. A. Schindler (1994), Practical example of the correction of Fourier-transform spectra for detector nonlinearity, *Appl. Opt.*, *33*(27), 6307–6314.

Ackerman, S. A., and K. I. Strabala (1994), Satellite remote-sensing of H_2SO_4 aerosol using the 8-μm to 12-μm window region: Application to Mount Pinatubo, *J. Geophys. Res.*, *99*(D9), 18,639–18,649.

Biermann, U. M., B. P. Luo, and T. Peter (2000), Absorption spectra and optical constants of binary and ternary solutions of H_2SO_4, HNO_3, and H_2O in the mid infrared at atmospheric temperatures, *J. Phys. Chem. A*, *104*(4), 783–793.

Boone, C. D., and P. F. Bernath (2003), SciSat-1 mission overview and status, in *SPIE Earth Observing Systems VIII*, edited by W. L. Barnes, pp. 133–142, Int. Soc. Opt. Eng., Bellingham, Wash.

Deshler, T., B. J. Johnson, and W. R. Rozier (1993), Balloonborne measurements of Pinatubo aerosol during 1991 and 1992 at 41°N: Vertical profiles, size distribution, and volatility, *Geophys. Res. Lett.*, *20*(14), 1435–1438.

Echle, G., T. von Clarmann, and H. Oelhaf (1998), Optical and microphysical parameters of the Mt. Pinatubo aerosol as determined from MIPAS-B mid-IR limb emission spectra, *J. Geophys. Res.*, *103*(D15), 19,193–19,211.

Eldering, A., F. W. Irion, A. Y. Chang, M. R. Gunson, F. P. Mills, and H. M. Steele (2001), Vertical profiles of aerosol volume from high-spectral-resolution infrared transmission measurements. I. Methodology, *Appl. Opt.*, *40*(18), 3082–3091.

Goodman, J., K. G. Snetsinger, R. F. Pueschel, G. V. Ferry, and S. Verma (1994), Evolution of Pinatubo aerosol near 19 km altitude over western North America, *Geophys. Res. Lett.*, *21*(12), 1129–1132.

Grainger, R. G., A. Lambert, F. W. Taylor, J. J. Remedios, C. D. Rodgers, M. Corney, and B. J. Kerridge (1993), Infrared absorption by volcanic stratospheric aerosols observed by ISAMS, *Geophys. Res. Lett.*, *21*, 1283–1286.

Grainger, R. G., A. Lambert, C. D. Rodgers, F. W. Taylor, and T. Deshler (1995), Stratospheric aerosol effective radius, surface-area and volume estimated from infrared measurements, *J. Geophys. Res.*, *100*(D8), 16,507–16,518.

Gunson, M. R., et al. (1996), The Atmospheric Trace Molecule Spectroscopy (ATMOS) experiment: Deployment on the ATLAS Space Shuttle missions, *Geophys. Res. Lett.*, *23*(17), 2333–2336.

Hervig, M. E., and T. Deshler (1998), Stratospheric aerosol surface area and volume inferred from HALOE, CLAES, and ILAS measurements, *J. Geophys. Res.*, *103*(D19), 25,345–25,352.

Hervig, M. E., J. M. Russell, L. L. Gordley, J. H. Park, S. R. Drayson, and T. Deshler (1996), Validation of aerosol measurements from the Halogen Occultation Experiment, *J. Geophys. Res.*, *101*(D6), 10,267–10,275.

Irion, F. W., et al. (2002), Atmospheric Trace Molecule Spectroscopy (ATMOS) experiment version 3 data retrievals, *Appl. Opt.*, *41*(33), 6968–6979.

Kahn, B. H., A. Eldering, F. W. Irion, F. P. Mills, B. Sen, and M. R. Gunson (2002), Cloud identification in Atmospheric Trace Molecule Spectroscopy infrared occultation measurements, *Appl. Opt.*, *41*(15), 2768–2780.

Kaye, J. A., and T. L. Miller (1996), The ATLAS series of shuttle missions, *Geophys. Res. Lett.*, *23*(17), 2285–2288.

Kent, G. S., D. M. Winker, M. T. Osborn, and K. M. Skeens (1993), A model for the separation of cloud and aerosol in Sage-II occultation data, *J. Geophys. Res.*, *98*(D11), 20,725–20,735.

Lambert, A., R. G. Grainger, J. J. Remedios, C. D. Rodgers, M. Corney, and F. W. Taylor (1993), Measurements of the evolution of the Mt. Pinatubo aerosol cloud by ISAMS, *Geophys. Res. Lett.*, *20*(12), 1287–1290.

Lambert, A., R. G. Grainger, J. J. Remedios, W. J. Reburn, C. D. Rodgers, F. W. Taylor, A. E. Roche, J. B. Kumer, S. T. Massie, and T. Deshler (1996a), Validation of aerosol measurements from the improved stratospheric and mesospheric sounder, *J. Geophys. Res.*, *101*(D6), 9811–9830.

Lambert, A., R. G. Grainger, H. L. Rogers, W. A. Norton, C. D. Rodgers, and F. W. Taylor (1996b), The H_2SO_4 component of stratospheric aerosols derived from satellite infrared extinction measurements: Application to stratospheric transport studies, *Geophys. Res. Lett.*, *23*(17), 2219–2222.

Lambert, A., R. G. Grainger, C. D. Rodgers, F. W. Taylor, J. L. Mergenthaler, J. B. Kumer, and S. T. Massie (1997), Global evolution of the Mt. Pinatubo volcanic aerosols observed by the infrared limb-sounding instruments CLAES and ISAMS on the Upper Atmosphere Research Satellite, *J. Geophys. Res.*, *102*(D1), 1495–1512.

Massie, S. T., P. L. Bailey, J. C. Gille, E. C. Lee, J. L. Mergenthaler, A. E. Roche, J. B. Kumer, E. F. Fishbein, J. W. Waters, and W. A. Lahoz (1994), Spectral signatures of polar stratospheric clouds and sulfate aerosol, *J. Atmos. Sci.*, *51*(20), 3027–3044.

Massie, S. T., T. Deshler, G. E. Thomas, J. L. Mergenthaler, and J. M. Russell (1996a), Evolution of the infrared properties of the Mount Pinatubo aerosol cloud over Laramie, Wyoming, *J. Geophys. Res.*, *101*(D17), 23,007–23,019.

Massie, S. T., et al. (1996b), Validation studies using multiwavelength cryogenic limb array etalon spectrometer (CLAES) observations of stratospheric aerosol, *J. Geophys. Res.*, *101*(D6), 9757–9773.

Niedziela, R. F., M. L. Norman, R. E. Miller, and D. R. Worsnop (1998), Temperature- and composition-dependent infrared optical constants for sulfuric acid, *Geophys. Res. Lett.*, *25*(24), 4477–4480.

Niedziela, R. F., M. L. Norman, C. L. DeForest, R. E. Miller, and D. R. Worsnop (1999), A temperature- and composition-dependent study of H2SO4 aerosol optical constants using Fourier transform and tunable diode laser infrared spectroscopy, *J. Phys. Chem. A*, *103*(40), 8030–8040.

Norton, R. H., and C. P. Rinsland (1991), ATMOS data processing and science analysis methods, *Appl. Opt.*, *30*(4), 389–400.

Oberbeck, V. R., E. F. Danielsen, K. G. Snetsinger, G. V. Ferry, W. Fong, and D. M. Hayes (1983), Effect of the eruption of El Chichon on stratospheric aerosol size and composition, *Geophys. Res. Lett.*, *10*(11), 1021–1024.

Rinsland, C. P., G. K. Yue, M. R. Gunson, R. Zander, and M. C. Abrams (1994), Midinfrared extinction by sulfate aerosols from the Mt. Pinatubo eruption, *J. Quant. Spectrosc. Radiat. Transfer*, *52*(3–4), 241–252.

Rinsland, C. P., et al. (1998), ATMOS/ATLAS 3 infrared profile measurements of clouds in the tropical and subtropical upper troposphere, *J. Quant. Spectrosc. Radiat. Transfer*, *60*(5), 903–919.

Rodgers, C. D. (1990), Characterization and error analysis of profiles retrieved from remote sounding measurements, *J. Geophys. Res.*, *95*(D5), 5587–5595.

Russell, P. B., et al. (1996), Global to microscale evolution of the Pinatubo volcanic aerosol derived from diverse measurements and analyses, *J. Geophys. Res.*, *101*(D13), 18,745–18,763.

Steele, H. M., A. Eldering, B. Sen, G. C. Toon, F. P. Mills, and B. H. Kahn (2003), Retrieval of stratospheric aerosol size and composition information from solar infrared transmission spectra, *Appl. Opt.*, *42*(12), 2140–2154.

Thibault, F., V. Menoux, R. LeDoucen, L. Rosenmann, J. M. Hartmann, and C. Boulet (1997), Infrared collision-induced absorption by O_2 near 6.4 μm for atmospheric applications: Measurements and empirical modeling, *Appl. Opt.*, *36*(3), 563–567.

Tisdale, R. T., D. L. Glandorf, M. A. Tolbert, and O. B. Toon (1998), Infrared optical constants of low-temperature H_2SO_4 solutions representative of stratospheric sulfate aerosols, *J. Geophys. Res.*, *103*(D19), 25,353–25,370.

Toon, O. B., M. A. Tolbert, B. G. Koehler, A. M. Middlebrook, and J. Jordan (1994), Infrared optical constants of H_2O ice, amorphous nitric-acid solutions, and nitric-acid hydrates, *J. Geophys. Res.*, *99*(D12), 25,631–25,654.

Zasetsky, A. Y., J. J. Sloan, R. Escribano, and D. Fernandez (2002), A new method for the quantitative identification of the composition, size and density of stratospheric aerosols from high resolution IR satellite measurements, *Geophys. Res. Lett.*, *29*(22), 2071, doi:10.1029/2002GL015816.

A. Eldering, M. R. Gunson, and F. W. Irion, Jet Propulsion Laboratory, California Institute of Technology, 4800 Oak Grove Drive, Mail Stop 183-601, Pasadena, CA 91109-8099, USA. (annmarie.eldering@jpl.nasa.gov)

B. H. Kahn and H. M. Steele, Department of Atmospheric and Oceanic Sciences, University of California at Los Angeles, Los Angeles, CA, USA.

F. P. Mills, Centre for Resource and Environmental Studies, Australian National University, Canberra, ACT, Australia.